

# Examining metal nanoparticle surface chemistry using hollow-core, photonic-crystal, fiber-assisted SERS

Fatemeh Eftekhari,<sup>1,†,\*</sup> Anna Lee,<sup>2,‡</sup> Eugenia Kumacheva,<sup>2</sup> and Amr S. Helmy<sup>1</sup>

<sup>1</sup>Department of Electrical and Computer Engineering, University of Toronto, 10 King's College Road, Toronto, Ontario M5S 3G4, Canada

<sup>2</sup>Department of Chemistry, University of Toronto, 80 Saint George Street, Toronto, Ontario M5S 3H6, Canada

\*Corresponding author: fatima.eftekhari@utoronto.ca

Received July 29, 2011; revised November 26, 2011; accepted December 21, 2011;  
posted December 21, 2011 (Doc. ID 151763); published February 14, 2012

In this Letter, we demonstrate the efficacy of hollow core photonic crystal fibers (HCPCFs) as a surface-enhanced Raman spectroscopy (SERS) platform for investigating the ligand exchange process on the surface of gold nanoparticles. Raman measurements carried out using this platform show the capability to monitor minute amounts of surface ligands on gold nanoparticles used as an SERS substrate. The SERS signal from an HCPCF exhibits a tenfold enhancement compared to that in a direct sampling scheme using a cuvette. Using exchange of cytotoxic cetyltrimethylammonium bromide with  $\alpha$ -methoxy- $\omega$ -mercaptopoly(ethylene glycol) on the surface of gold nanorods as an exemplary system, we show the feasibility of using HCPCF SERS to monitor the change in surface chemistry of nanoparticles. © 2012 Optical Society of America

OCIS codes: 240.6695, 060.5295, 280.4788, 240.6680.

Gold nanoparticles (NPs) have a broad range of applications owing to their intrinsic electromagnetic and chemical properties. In particular, gold NPs are used as surface-enhanced Raman spectroscopy (SERS) substrates for biomedical applications [1,2].

SERS addresses a number of limitations of fluorescence-based sensing of analytes, such as photobleaching, a broad emission spectrum of organic dyes hindering multiplexing, and insufficient quantification and sensitivity [2,3]. The root cause behind the high sensitivity achieved by SERS arises from the enhancement of the local electromagnetic field of metal NPs due to excitation of localized surface plasmons [1,4].

Modifying the surface of NPs with mixtures of ligands is essential in rendering NPs functional, stable, and target specific. In particular, a thorough understanding of the surface chemistry of gold NPs is fundamental to their efficient application in materials science and biomedical fields. Using gold NPs as a biological SERS probe requires control of their surface chemistry in order to make them biologically compatible. For example, because as-synthesized gold nanorods are coated with cytotoxic cetyltrimethylammonium bromide (CTAB), an exchange with biocompatible ligands is required [5].

Current methods used to identify the presence of surface ligands on NPs include fluorescence displacement methods, Fourier transform IR, reflection absorption IR spectroscopies, contact angle measurements, and transmission electron microscopy [6,7]. These techniques are either destructive or have insufficient sensitivity for low concentrations of surface ligands. Although SERS measurements conducted for colloidal gold NPs offer a sensitive and a nondestructive alternative technique, full exploitation of local electric field enhancement is commonly achieved using aggregates of gold NPs. In addition, using low concentrations of NPs in a solution can be challenging due to the associated poor signal-to-noise ratio. In order to overcome these barriers, enhanced analytical approaches are needed.

Hollow core photonic crystal fibers (HCPCF) serve as a promising platform for various sensing applications.

The waveguide characteristics and the accessibility to the hollow cladding channels of HCPCF have opened up many possibilities for chemical and biochemical sensing utilizing fluorescence [8], Raman scattering [9–12], and SERS [13–15]. The utilization of HCPCF can result in the enhancement of the Raman signal strength by approximately 2 orders of magnitude [16]. Initial SERS measurements in HCPCF have been conducted by incorporating colloidal solutions of Au or Ag NPs either by being coated on the inner surface of the fiber hollow channels or mixed with a solution and filled in a limited segment of the HCPCF [13–15]. These studies show that, in addition to significantly higher sensitivity, SERS in HCPCF can also provide a nondestructive and direct route to identifying the presence of minute amounts of ligand adsorbed on the surface of gold NPs. In this Letter, we show the exquisite performance of HCPCF as an SERS probe to monitor a ligand exchange process on the surface of NPs by investigating PEGylation of colloidal nanorods (NRs) at extremely low concentration that is otherwise not detectable via a direct solution sampling.

The schematic diagram of the experimental setup is shown in the inset of Fig. 1(b). The excitation source is a 632 nm HeNe laser in conjunction with a JY Horiba HR800 LabRam Raman spectrometer. The excitation light is coupled into the core of HCPCF from the top end through an objective lens, while the other end of the HCPCF is immersed into the solution of NPs. The cladding holes are sealed at the probing end of the fiber using the fusion splicing technique. As such, the solution studied only fills the central core of the fiber via capillary forces. The periodic cladding holes confine the excitation laser inside the core of the HCPCF through both photonic band-gap effects and total internal reflection. The well-confined excitation interacts directly with the sample molecules while propagating along the length of the HCPCF. The backscattered Raman from the sample propagates through the fiber back to the top end and is collected through the same objective lens. The 50 $\times$  objective is chosen due to its NA that best matches that of the HCPCF to provide maximum coupling efficiency and sensitivity.

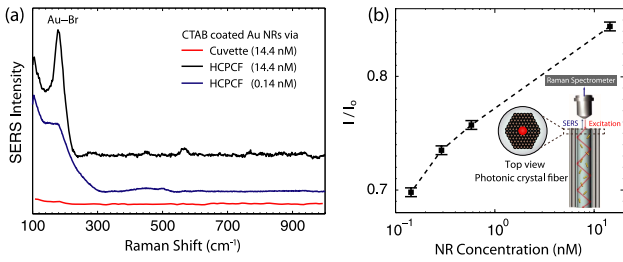


Fig. 1. (Color online) (a) SERS spectra of CTAB-coated gold NRs detected through direct sampling in a cuvette and core-filled HCPCF. (b) Variation in the normalized SERS peak intensity measured at  $178\text{ cm}^{-1}$  plotted as a function of concentration of CTAB-coated gold NRs (the concentration of the NRs was determined by extinction measurements [17]). SERS variation ( $y$  error) is based on three measurements.

The HCPCF (Crystal Fiber Model HC1060) has a  $9.5\text{ }\mu\text{m}$  diameter core, surrounded by a silica microstructured cladding with an air fill fraction  $>90\%$ . The wavelength regime, where photonic bandgap guiding is present for this fiber, coincides with the HeNe laser wavelength when it is filled with aqueous solutions. Minimal interference from the Raman spectrum of the silica of the HCPCF is observed. All the measurements reported here were carried out using  $7.0\text{ cm}$  long segments of HCPCF. CTAB-coated gold NRs with an average length and width of  $38.42 \pm 2.69$  and  $8.75 \pm 0.61\text{ nm}$ , respectively, were prepared by the method reported elsewhere [18] and used as an SERS substrate. Transverse and longitudinal localized surface plasmon resonance wavelengths were centered at  $510$  and  $773\text{ nm}$ , respectively.

Figure 1(a) shows SERS spectra of the  $14.4\text{ nM}$  aqueous solution of the NRs obtained by focusing the laser beam onto the core of a core-filled HCPCF or by focusing the laser beam directly into the NRs solution in a cuvette. The detected signal from HCPCF is nearly 40 times stronger than that from the direct sampling of the NRs in the cuvette. The strong peak centered at  $178\text{ cm}^{-1}$  was attributed to the Au-Br vibrational mode that originates from the CTAB capping molecules of gold NRs. We used this Raman mode to determine the limit of detection of SERS in HCPCF that was found to be  $0.14\text{ nM}$  for the solution of CTAB-coated gold NRs [Fig. 1(b)].

Adsorption of the dye Congo Red ( $3\text{ }\mu\text{M}$ ) on the NRs was used to examine SERS enhancement in HCPCF. A and B in Fig. 2 show the SERS spectra of Congo Red, which were acquired from the core-filled HCPCF and from the NR solution placed in the cuvette. In order to verify that the detected signal is caused by SERS rather than conventional spontaneous Raman scattering, a Raman spectrum of Congo Red of  $564\text{ }\mu\text{M}$  was acquired, as can be seen at C in Fig. 2. No discernible vibrational modes of Congo Red were detected from that Raman spectrum.

A comparison of the spectra presented in Fig. 2 shows that, with the use of HCPCF, the noise level was considerably reduced and well-resolved Raman modes of Congo Red were revealed. The resolved peaks of Congo Red matched its characteristic peaks [19]. In addition, the peak height of the  $1167\text{ cm}^{-1}$  Raman mode obtained from the SERS in HCPCF was enhanced tenfold compared to the spectrum acquired by direct sampling in the cuvette.

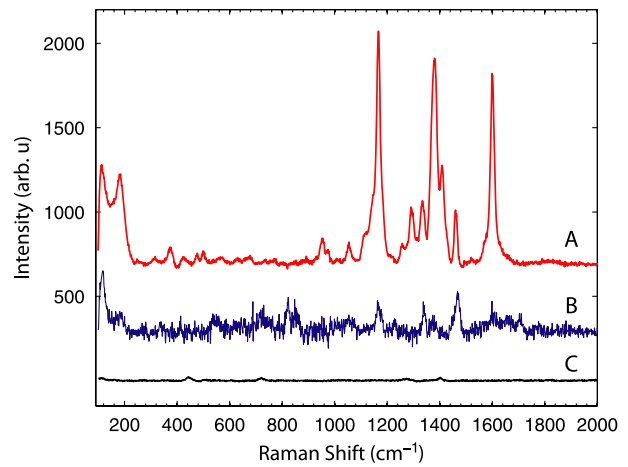


Fig. 2. (Color online) SERS spectra of  $3\text{ }\mu\text{M}$  Congo Red molecules by using core-filled HCPCF (A), direct sampling from a cuvette (B). Ordinary Raman spectrum of Congo Red molecules at the concentration of  $564\text{ }\mu\text{M}$  (C). The spectra have been separated vertically for clarity.

We have examined the root causes of the signal enhancement in previous studies [10,12,16]. The enhancement in the detected Raman signal is due to the increased interaction length and efficient collection of the Raman scattering signal via the bandgap effect over this extended interaction length. By confining both the excitation laser and the liquid sample along the length of the HCPCF, a larger length for light-matter interaction is achieved compared to that associated with the conventional Raman spectroscopy scheme. In direct sampling, the excitation laser is focused directly into the NR solution; therefore, the effective interaction volume is limited by the spot size of the pump laser and the depth of field. Raman scattering is omnidirectional, and due to the limited NA of the collecting objective lens, in this scheme only a fraction of the scattered Raman signal could be collected. Since the scattered Raman wavelengths were only slightly shifted from the excitation laser wavelength, with the use of HCPCF, Raman signal propagation was also confined inside the central core of the fiber and was collected more efficiently by the objective lens. The collection efficiency of HCPCF can be viewed as the solid angle that collects the Raman signal inside the fiber. It is governed by the NA of the fiber or the refractive index difference between the core and the cladding. Since the effective refractive index of HCPCF cladding is close to 1, greater collection angle is obtained from HCPCF in comparison with the regular capillary waveguides, such as Teflon capillary tubes.

To further examine the sensitivity of the proposed HCPCF SERS platform, we investigated a ligand exchange process on the surface of NRs by replacing CTAB with  $\alpha$ -methoxy- $\omega$ -mercaptopoly(ethylene glycol) (SH-mPEG) (molecular weight  $12,000\text{ g/mol}$ ). Gold NRs are considered to be a suitable candidate as an SERS probe and plasmonic sensor for biological applications due to the spectral position of the localized surface plasmon resonance, which is located in the near-IR region. However, CTAB is cytotoxic, requiring ligand exchange with biocompatible ligands for applications in biology [20]. For

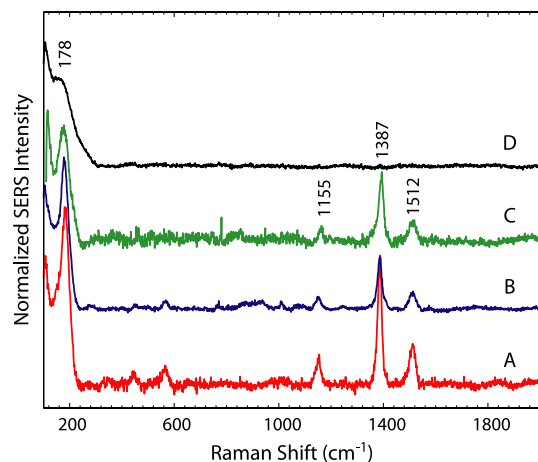


Fig. 3. (Color online) Normalized SERS spectra of CTAB-coated gold NRs as a function of SH-mPEG concentration: control (A), 20  $\mu\text{M}$  of PEG (B), 50  $\mu\text{M}$  of PEG (C), 100  $\mu\text{M}$  of PEG (D). The peak at 103  $\text{cm}^{-1}$  was used to normalize the peaks. The spectra have been separated vertically for clarity.

example, replacement of CTAB with SH-mPEG provides biocompatibility, reduced enzymatic degradation, nonimmunogenicity, and stability in both highly ionic media and in the blood circulation system [21]. Surface CTAB replacement occurs owing to chemisorption of the thiol moiety of poly(ethylene glycol) (PEG) (the binding energy of Au-S is approximately 167  $\text{kJ mol}^{-1}$  [22]).

Figure 3 shows the variation of SERS spectra of CTAB as a function of the concentration of SH-mPEG in solution. The solution of SH-mPEG (with the concentrations of 20, 50, and 100  $\mu\text{M}$ ) was introduced into the solution of CTAB-coated gold NRs so that the final concentration of the NRs was maintained at 0.54 nM. In contrast to other techniques, we emphasize that this extremely low concentration of NRs is not detectable via direct solution sampling methods due to poor signal-to-noise ratio. Further, the minute amounts of solution (sampling volume is approximately  $5 \times 10^{-6} \text{ cm}^3$ ) that can be analyzed may offer advantages in biological sensing including forensics. By using this fiber methodology, there is a potential for portable sensing and ultracompact devices.

Figure 3 shows that, as the concentration of SH-mPEG increased, the intensities of CTAB Raman modes at 178, 1155, 1387, and 1512  $\text{cm}^{-1}$  sequentially decreased, indicating the gradual replacement of the CTAB capping layer by the SH-mPEG polymer. This result demonstrates the capability of the HCPCF SERS probe to effectively monitor the presence of the minute amounts of ligands on the surface of NRs that cannot be detected using direct solution sampling. We estimated that the surface area of an individual NR is 1300  $\text{nm}^2$ , based on the assumption that the NR has two hemispheres on the ends of the cylinder. The area per molecule of CTAB and SH-mPEG (assuming a brushlike configuration) is 0.22 and 10.8  $\text{nm}^2$ , respectively [23]. Therefore, each NR would contain approximately  $12 \times 10^3$  CTAB (assuming a bilayer) and  $1.2 \times 10^2$  PEG molecules on its surface, representing  $3.6 \times 10^{18}$  CTAB and  $3.6 \times 10^{16}$  PEG molecules at a 0.5 nM concentration of the NRs.

In this Letter, we demonstrated an efficient platform for SERS using core-filled HCPCF. We achieved a tenfold enhancement in the SERS signal in HCPCF compared to that achieved by direct sampling in cuvette. Therefore, this platform can be used as a useful method for ultrasensitive detection of vibrational modes of chemical and biological molecules. The great potential of HCPCF for optical sensing originates from the increased light-matter interaction volume and the efficient collection of the SERS scattering along the extended length of the HCPCF. Using exchange of CTAB with SH-mPEG on the surface of gold NRs as an exemplary system, we showed the feasibility of using HCPCF SERS to monitor the change in surface chemistry of NPs, which can be extended to studies of *in situ* cytotoxicity of different kinds of NPs.

†These authors contributed equally to this work.

## References

1. R. Aroca, *Surface-Enhanced Vibrational Spectroscopy* (Wiley, 2006).
2. R. A. Alvarez-Puebla and L. M. Liz-Marzan, *Small* **6**, 604 (2010).
3. J. R. Baena and B. Lendl, *Curr. Opin. Chem. Biol.* **8**, 534 (2004).
4. M. Moskovits, *J. Raman Spectrosc.* **36**, 485 (2005).
5. T. S. Hauck, A. A. Ghazani, and W. C. W. Chan, *Small* **4**, 153 (2008).
6. L. M. Demers, C. A. Mirkin, R. C. Mucic, R. A. Reynolds, R. L. Letsinger, R. Elghanian, and G. Viswanadham, *Anal. Chem.* **72**, 5535 (2000).
7. L. Li, Q. Mu, B. Zhang, and B. Yan, *Analyst* **135**, 1519 (2010).
8. S. Smolka, M. Barth, and O. Benson, *Opt. Express* **15**, 12783 (2007).
9. S. O. Konorov, C. J. Addison, H. G. Schulze, R. F. B. Turner, and M. W. Blades, *Opt. Lett.* **31**, 1911 (2006).
10. S. A. Rutledge, A. A. Farah, J. Dinglasan, D. J. Anderson, A. Das, J. Goh, C. Goh, and A. S. Helmy, *J. Phys. Chem. C* **113**, 20208 (2009).
11. R. M. Abu-Ghazalah, J. Irizar, A. S. Helmy, and R. B. Macgregor, Jr., *Biophys. Chem.* **147**, 123 (2010).
12. J. S. W. Mak, A. A. Farah, F. Chen, and A. S. Helmy, *ACS Nano* **5**, 3823 (2011).
13. X. Yang, C. Shi, D. Wheeler, R. Newhouse, B. Chen, J. Z. Zhang, and C. Gu, *J. Opt. Soc. Am. A* **27**, 977 (2010).
14. C. Shi, C. Lu, C. Gu, L. Tian, R. Newhouse, S. Chen, and J. Z. Zhang, *Appl. Phys. Lett.* **93**, 153101 (2008).
15. Y. Han, S. L. Tan, M. K. K. Oo, D. Pristiniski, S. Sukhishvili, and H. Du, *Adv. Mater.* **22**, 2647 (2010).
16. F. Eftekhari, J. Irizar, L. Hulbert, and A. S. Helmy, *J. Appl. Phys.* **109**, 113104 (2011).
17. C. J. Orendorff and C. J. Murphy, *J. Phys. Chem. B* **110**, 3990 (2006).
18. B. Nikoobakht and M. A. El-Sayed, *Chem. Mater.* **15**, 1957 (2003).
19. A. Elhaddaoui, A. Delacourte, and S. Turrell, *J. Mol. Struct.* **294**, 115 (1993).
20. T. S. Hauck, A. A. Ghazani, and W. C. W. Chan, *Small* **4**, 153 (2008).
21. A. S. Karakoti, S. Das, S. Thevuthasan, and S. Seal, *Angew. Chem. Int. Ed.* **50**, 1980 (2011).
22. L. H. Dubois and R. G. Nuzzo, *Annu. Rev. Phys. Chem.* **43**, 437 (1992).
23. S. C. Boca and S. Astilean, *Nanotechnology* **21**, 235601 (2010).